

Article

Application of Algal Nanotechnology for Leather Wastewater Treatment and Heavy Metal Removal Efficiency

Sheza Ayaz Khilji ¹, Neelma Munir ², Irfan Aziz ³, Bareera Anwar ¹, Maria Hasnain ², Ali Murad Jakhar ⁴, Zahoor A. Sajid ⁵, Zainul Abideen ^{3,*}, Muhammad Iftikhar Hussain ⁶, Abeer A. El-Habeeb ⁷ and Hsi-Hsien Yang ^{8,*}

- ¹ Department of Botany, Division of Science and Technology, University of Education, Lahore 54770, Pakistan
- ² Department of Biotechnology, Lahore College for Women University, Lahore 35200, Pakistan
- ³ Dr. Muhammad Ajmal Khan Institute of Sustainable Halophyte Utilization, University of Karachi, Karachi 75270, Pakistan
- ⁴ Institute of Plant Sciences, University of Sindh, Jamshoro 76080, Pakistan
- ⁵ Institute of Botany, University of the Punjab, Lahore 54590, Pakistan
- ⁶ Department of Plant Biology and Soil Science, Universidad de Vigo, Campus Lagoas Marcosende, 36310 Vigo, Spain
- ⁷ Department of Chemistry, College of Science, Princess Nourah bint Abdulrahman University, P.O. Box 84428, Riyadh 11671, Saudi Arabia
- ⁸ Department of Environmental Engineering and Management, Chaoyang University of Technology, No. 168, Jifeng E. Rd., Wufeng District, Taichung 413310, Taiwan
- * Correspondence: zuabideen@uok.edu.pk (Z.A.); hhyang@cyut.edu.tw (H.-H.Y.)

Citation: Khilji, S.A.; Munir, N.; Aziz, I.; Anwar, B.; Hasnain, M.; Jakhar, A.M.; Sajid, Z.A.; Abideen, Z.; Hussain, M.I.; El-Habeeb, A.A.; et al. Application of Algal Nanotechnology for Leather Wastewater Treatment and Heavy Metal Removal Efficiency. *Sustainability* **2022**, *14*, 13940. <https://doi.org/10.3390/su142113940>

Academic Editor: Agostina Chiavola

Received: 26 September 2022

Accepted: 24 October 2022

Published: 26 October 2022

Publisher's Note: MDPI stays neutral with regard to jurisdictional claims in published maps and institutional affiliations.



Copyright: © 2022 by the authors. Licensee MDPI, Basel, Switzerland. This article is an open access article distributed under the terms and conditions of the Creative Commons Attribution (CC BY) license (<https://creativecommons.org/licenses/by/4.0/>).

Abstract: Wastewater from tanneries may ruin agricultural fields by polluting them with trace metals. The synthesis of nanoparticles (NPs) from algal sources and their application could help in decreasing hazardous materials, for environmental safety. The potential of zinc oxide nanoparticles made from *Oedogonium* sp. was evaluated for removal of heavy metals from leather industrial wastewater. Synthesized algal nanoparticles (0 (control), 0.1, 0.5, and 1 mg) were applied to treat wastewater by using different concentrations of leather industrial effluents (0%, 5%, 10%, 15%, and 100%) for 15, 30, and 45 d. The wastewater collected was dark brown to black in color with very high pH (8.21), EC (23.08 $\mu\text{s}/\text{cm}$), and TDS, (11.54 mg/L), while the chloride content was 6750 mg/L. The values of biological oxygen demand (BOD) and chemical oxygen demand (COD) ranged between 420 mg/L and 1123 mg/L in the current study. Prior to the application of nanoparticles, Cr (310.1), Cd (210.5), and Pb (75.5 mg/L) contents were higher in the leather effluents. The removal efficiency of TDS, chlorides, Cr, Cd, and Pb was improved by 46.5%, 43.5%, 54%, 57.6%, and 59.3%, respectively, following treatment with 1 mg of nanoparticles after 45 d. Our results suggested that the green synthesis of ZnO nanoparticles is a useful and eco-friendly biotechnological tool for treating tannery effluents, before they are discharged into water bodies, thus making the soil environment clean.

Keywords: bioremediation; green synthesis; *Oedogonium* sp.; nanoparticles; wastewater treatment; environmental protection

1. Introduction

The contamination of soil with wastewater has become a global problem over the last few decades, along with increases in the demands on the food and water supply [1]. Natural processes such as weathering and volcanic eruptions are the main source of heavy metal accumulation in the environment [2]. However, exposure to synthetic fertilizers and

heavy metal discharge via anthropogenic activities have become a major threat to the environment [3]. Wastewater pollution has increased at an alarming rate due to the suboptimal discharge of effluents from rapidly increasing global industrialization [4]. Different units and industrial pools (chemical, cement, leather, textile steel, petrochemical, food processing, construction, rubber manufacturing, crockery, publishing, and paper printing) produce pollutants that are released into the wastewater [5]. However, the discharged wastewater of different industries is the major source of soil metal pollution such as iron (Fe^{2+}), cobalt (Co^{2+}), nickel (Ni^{2+}), cadmium (Cd^{2+}), zinc (Zn^{2+}), lead (Pb^{2+}), copper (Cu^{2+}), chromium (Cr^{2+}), mercury (Hg^{2+}), molybdenum (Mo^{2+}), and selenium (Se^{2+}) [6]. Discharged wastewater is directly ruining agricultural fields, as the harmful chemicals as well as pollutants released by industrial units into nearby drains have caused drastic effects that alter the sustainability of the ecosystem. Heavy metals are the elements with an atomic weight between 63 and 200 and a specific gravity greater than 4. The specific gravity of these metal ions is five times greater than those of water bodies. Trace amounts of some metals are required by living organisms; however, any excess amount of these metals can be detrimental to organisms [7]; hence, pollution monitoring and trace metal eradication are essentially needed. Moreover, the application of nanomaterials is of great importance for phytoremediation, improve crop production and ecosystem restoration [8], as NPs may interact with pollutants in water and absorb them due to their special physicochemical properties: being nanosized, having a large specific surface area, and being potentially efficient carriers for many pollutants including heavy metals and organic pollutants [9].

It is estimated that the well-being of humans is affected due to heavy metal intrusion in water and vegetables grown under wastewater. In Karachi alone, >6000 industrial units discharge about 300 million gallons of industrial waste/day, which are dumped in the coastal areas affecting living beings in the ocean [10], as the accumulation of heavy metals in fish (iron clogging in fish gills), marine birds, and seaweeds has resulted in their increased mortality and, ultimately, has disrupted the process of the food chain [9]. Almost 10% of the total dyes used in textile industries are disposed as wastewater and are one of the major causes of water pollution [11]. The effluents from industries are complex, containing a wide variety of dye products (such as dispersants, acids, bases, salts, detergents, and oxidants), and the discharge of these colored effluents goes into rivers and lakes [12]. The excessive exposure of heavy metals (arsenic (As), lead (Pb), cadmium (Cd), zinc (Zn), and copper (Cu)) in discharge areas and agricultural land also causes a negative impact on marine organisms, cultivated crops, and ultimately human beings through the food chain [13]. The above-mentioned problems warrant proper treatment of wastewater effluents prior to their final discharge into the environment, particularly for large water bodies. Not a single industrial sector has paid any attention toward the predischage treatment of wastewater. Industrial as well as sewage effluents are usually discharged into agricultural areas, where wastewater is used for the purpose of irrigation. It not only poses a harmful effect on the soil surface and its characteristics but also affects the quality of crops. About 20% of the irrigation in Pakistan uses untreated wastewater [14]. Crops that are being irrigated by wastewater accumulate large concentrations of heavy metals. Metal ions are attached to the negatively charged soil particles, and when cations detach from soil particles, they are freely available and adsorbed by plants via water uptake [15]. A variety of contaminated crops are consumed by people, which becomes a major route for heavy metals to enter the human body via the food chain, causing serious health hazards [16]. A variety of toxins present in industrial waste alters soil properties and the crop yield, besides affecting the human immune system [4]. Toxic pollutants also negatively affect aquatic life. The accumulation of heavy metals and other toxins in fish (iron clogging in fish gills), marine birds, and seaweeds has increased mortality and has ultimately disrupted the process of the food chain [17].

Nanotechnology is a promising field to treat wastewater contaminants in a reliable and cost-effective manner. Bioremediation process is carried out with the help of different

types of NPs, which can adsorb effluents (heavy metals) from contaminated water [18]. In the fields of environmental science and technology, nanomaterials are identified as effective substances due to their large surface area, high thermal resistance and capacity, very small size, self-assembly, and high chemical reactivity [19]. The basic metallic NMs are metal oxides, quantum dots and noble nanomaterials. Due to their small size, they show a significant change in their atomic structure and magnetic characteristics. Different nanoscale materials have a large surface area, a size within 1–100 nm (means one-billionth of a material) [20], and physicochemical characteristics with a notable impact in lowering the concentration of pollutants, especially heavy metals from wastewater [21]. Nanoparticles synthesized by algae are a very simple, cost-effective, and time-saving method [22]. Algae are known to have potential as a suitable biosorbent because of their fast and easy growth as well as their widespread availability [23]. Algal extract contains a variety of pigments, polysaccharides, proteins, and peptides along with a functional group [24] that acts as a reducing agent and reduces the metals' ions at optimal conditions, without producing any toxic byproducts [25]. The sorption capability of algae has been attributed to their cell walls, which are often porous and allow for the passage of molecules and ions in aqueous solutions. Nanoparticles synthesized by microalgae have gained lot of interest, since they can bioremediate toxic metals, further converting them to more amenable forms [26].

The treatment of polluted water is the leading application of nanotechnology. Different nanomaterials including nanotubes, magnetic nanoparticles, a variety of nanofilter membranes, metal oxide NPs, and nanosensors help to isolate heavy metals in polluted water [27]. Some studies on nanoparticles have been conducted on wastewater treatment in conventional activated sludge (CAS) processes [28]. The activated charged functional groups on the surface area of NPs have a great affinity to adsorb metallic ions. With the passage of time, the demand for NPs due to their superb adsorption ability has increased [29]. They are currently applied in different industries including the biomedical field (acting as antimicrobial, drug delivery, biosensing, biomarker mapping, molecular imaging, targeted therapy, and antitumor agents) [30]. The green synthesis of ZnO nanoparticles has increased the demand for these nanomaterials because of their ecofriendly nature, cost-effectivity, and time- and energy-saving process compared to other conventional physicochemical processes [31]. An agricultural area that is continuously irrigated with wastewater bears a consistently higher concentration of toxic pollutants. There are 16%–68.4% protein content decreases due to the toxicity of cadmium in maize [32]. It also influences the nitrogen concentration in different tissues of the plant. These contaminants affect the microbial community in soil very badly, disturb ecological processes, and ultimately result in stunted growth and decreased crop yields [33]. In view of the different advantages of NPs, the aim of the present study was to assess the ability of ZnO-algal-synthesized nanoparticles to reduce heavy metal content and to lower down the concentration of other pollutants in wastewater. We hypothesized that the removal efficiency of toxic waste using an algal nanoparticle would increase with time and dosage. The following questions were addressed in this study: (1) What concentration of algal-synthesized nanoparticles would be effective in removing trace metals from wastewater? (2) Does the removal efficiency of toxic waste increase with the passage of time?

2. Methodology

2.1. Wastewater Collection, Algal Sampling, and Its Identification

The wastewater was collected from Sundar Industrial Estate, Punjab, Pakistan (Figure 1). The collected wastewater was dark in color and had pungent smell. The algae were collected from freshwater ponds located near the main GT Road, Muridke, Pakistan (Figure 1). Algal species were identified on the basis of morphology under a microscope and by comparing sequences of their partial 18S rDNA and internal transcribed spacer (ITS) region [34]. DNA was extracted using the CTAB method [35]. The 18S rDNA gene was

amplified by PCR (Meradd ICCC—MPTC02077), and PCR products were sequenced by the service provider Macrogen. The resultant sequences were compared to existing sequences using BLAST tool (<https://blast.ncbi.nlm.nih.gov/Blast.cgi>, accessed on 10 July 2022). Multiple sequences were aligned using ClustalW in the Molecular Evolutionary Genetic Analysis tool (MEGAX software). Phylogenetic trees were constructed using the neighbor-joining method and 1000 bootstrap re-samplings, and their respective nucleotide sequences were submitted to NCBI.



Figure 1. Wastewater and algal Collection.

2.2. Green Synthesis of Zinc Oxide Nanoparticles from Algae

2.2.1. Algae Extract

Algal samples were washed with distilled water for removing the adhered particles. They were dried in a shaded place. The dried algal material was powdered, weighed, and stored in clean containers. Washed algal biomass (2 g) was mixed with 100 mL of distilled water and kept in a water bath for 20 min at 80 °C. The algal extracts were then filtered through Whatman's No. 1 filter to obtain the algal extract solution [36].

2.2.2. Salt Solution

The algal extract solution was used for the reduction of zinc acetate monohydrate salt to ZnO-NPs. The 0.5 M salt solution was prepared by adding 7.17 g $\text{ZnSO}_4 \cdot 7\text{H}_2\text{O}$ in 50 mL of dH_2O . The algal extract was gradually added in salt solution with continuous stirring. The change in color of the solutions was monitored. The solution was kept in ambient temperature (37 °C) for 24 h in a shaking incubator at 120 rpm. The solution was then centrifuged at 6000 rpm for 30 min. The pellet was collected and centrifuged again at 6000 rpm for 30 min. This process was repeated thrice to remove remains of unreacted algal extract and zinc acetate. The pellet was finally dried in an oven [37].

2.2.3. Optimizing Factors of Zinc Oxide Nanoparticles (ZnO-NPs) Synthesis

The physical and chemical factors affecting the production as well as the distribution of ZnO-NPs were optimized. Different factors such as temperature, pH, contact time, and salt concentration were investigated by detecting maximum surface plasmon resonance by a UV–Vis spectrophotometer. The different contact times (6, 12, 24, 36, 48, and 72 min) between algal biomass filtrate and zinc acetate monohydrate salt were assessed. Moreover, the incubation temperatures (25 °C, 30 °C, 35 °C, and 40 °C), different pH values (5, 6, 7, 8, and 9), and different concentrations of salt (0.1–0.25 mM) were assessed. At the end of each experiment, 1.0 mL of the sample was withdrawn to measure the color intensity at maximum SPR at $\lambda_{\text{max}} = 300 \text{ nm}$ [38].

2.2.4. Characterization of ZnO-NPs by UV

Color changes in the mixture of algal extract/ ZnSO_4 solutions were measured by spectrophotometry (JENWAY 6305 Spectrophotometer, 230 V/50 Hz, Staffordshire, UK),

at wavelengths ranging between 200–800 nm. Bioreduction of zinc acetate in aqueous solution was monitored (color change) by double beam UV–Vis spectrophotometer at different wavelengths (ranging 200–800 nm). The bioreduced zinc sulphate was purified for further characterization studies by putting it in centrifugation at 6000 rpm for 30 min. The pellet was collected and washed in sterile double-distilled water to get free of any biological molecule present in the algal extract [39].

2.2.5. Characterization of ZnO-NPs by FTIR

The functional groups present in green synthesized ZnO-NPs were analyzed by FT-IR analysis. About 0.2 g of ZnO-NPs powder was loaded onto a disc at high pressure. The FT-IR spectra were scanned at a resolution of 4.0 cm^{-1} at a wavelength of $500\text{--}4000\text{ cm}^{-1}$. Fourier transform infrared (FT-IR) spectroscopy (Agilent Cary 660 FT-IR model) was used to inspect the functional groups present in the fungal biomass filtrate and involved in the reduction and stabilization of ZnO-NPs. The ZnO-NP sample was mixed with KBr and scanned in the range of $400\text{ to }4000\text{ cm}^{-1}$ [40].

2.2.6. Characterization of ZnO-NPs by SEM

SEM at 5 kV, magnification $\times 10\text{ k}$, was used to examine the morphology of the synthesized ZnO-NPs. The sample film was prepared on a carbon-coated copper grid by simply dropping the suspension of ZnO-NPs in water on the grid, the excess solution was removed with blotting paper, and the film on the SEM grid was allowed to dry for 5 min under a mercury lamp. The surface images of the samples were captured at various magnifications. By focusing on the primary electron beam and detecting secondary or backscattered electron signals, SEM produces high-resolution images of samples [41].

2.3. Treatment of Wastewater with Nanoparticles

Three replicates along with control (0%) (no effluent) were used for the treatment of leather industry effluents. The experiment was carried out in 250 mL of jars with three replicates (R1, R2, and R3), and each analyzed at different time intervals i.e., 15, 30, and 45 d. Different concentrations of collected samples were treated with the four concentrations of nanoparticles 0 (control), 0.1, 0.5, and 1.0 mg, respectively, along with the control (Table 1). Following parameters were analyzed for all samples: three different concentrations along with control (0%) were prepared using distilled water for the leather industry effluents according to the requirement of the experiment: 0% (contained only distilled water), 5% (5 mL of effluent in 95 mL of dH₂O), 10% (10 mL of effluent in 90 mL of dH₂O), 15% (15 mL of effluent in 85 mL of dH₂O), and 100% (pure industrial wastewater).

Table 1. Total concentrations of industrial effluents along with their replicates and treatment of nanoparticles.

Treatment of Nanoparticles	Effluent Concentration				Total Replicates
	0%	5%	10%	15%	
0 mg	R1	R1	R1	R1	48
	R2	R2	R2	R2	
	R3	R3	R3	R3	
0.5 mg	R1	R1	R1	R1	
	R2	R2	R2	R2	
	R3	R3	R3	R3	
1 mg	R1	R1	R1	R1	
	R2	R2	R2	R2	
	R3	R3	R3	R3	
1.5 mg	R1	R1	R1	R1	
	R2	R2	R2	R2	
	R3	R3	R3	R3	

2.4. Analysis of Effluents to Evaluate the Bioremediation Potential of ZnO Nanoparticles

The pH (acidity or alkalinity), EC (electric conductivity), and TDS (total dissolved solids) of the collected sample were determined with the help of HI-9811-5 pH/EC/TDS/°C portable meter (HANNA Instruments, Cecili, Italy). Chlorides, chemical oxygen demand (COD), and biological oxygen demand were determined by the testing standard was based on the *Standard Methods for the Examination of Water and Wastewater* [41].

Atomic absorption spectrophotometer (GBC SAVAANT AA Australia) was used to estimate heavy metal concentration by acid digestion of effluents. Then, 5 mL of HNO₃ and 15 mL of perchloric acid was added in 25 mL of effluents with ratio of 3:1. The final volume was raised up to 100 mL by adding the distilled water. Then, the solution was filtered with filter paper. Finally, the filtrate solution was used for the determination of heavy metal concentration in sample [42].

To check the significance level of observed means for all selected parameters, the data were statistically analyzed by using statistical software COSTAT v 6.303 (Cohort software, Monterey, California). One-way and two-way ANOVA was applied followed by LSD test.

3. Results

3.1. Algae Identification

Algal sample in this study was obtained from ponds and selected for NP synthesis. The selected strain was primarily identified with the help of microscopic studies that were based on morphology. The selected strain appeared dull green, multicellular, and unbranched filamentous and was 4–54 µm in diameter. Morphological characterization indicated the algal strains as *Oedogonium* sp., which was later confirmed by the amplification of internal transcribed spacer (ITS) gene. The sequence analysis strongly revealed the algal strain as *Oedogonium* sp. (Figure 2) (<https://www.ncbi.nlm.nih.gov/>, accessed on 10 July 2022).

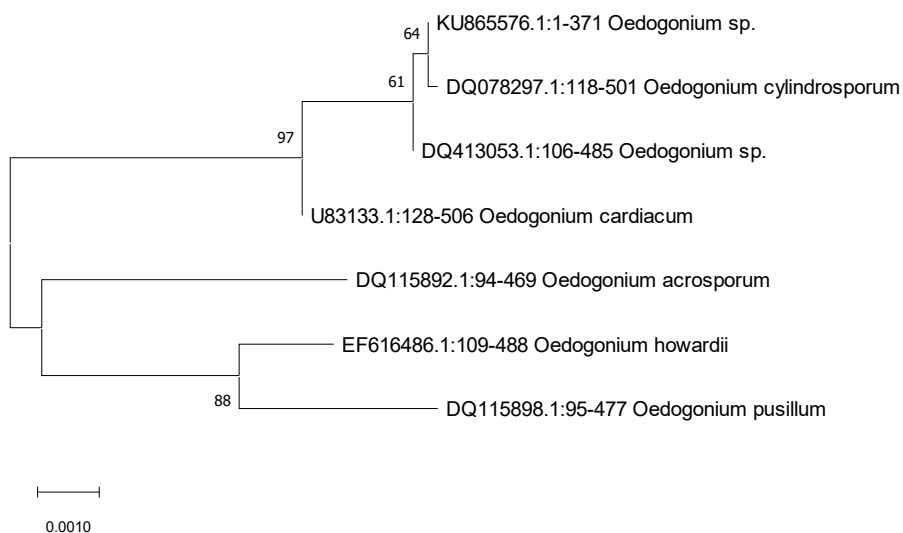


Figure 2. Phylogenetic tree of *Oedogonium* sp. using the neighbor-joining method.

3.2. Nanoparticle Synthesis

3.2.1. Optimizing Factors of Zinc Oxide Nanoparticles (ZnO-NPs) Synthesis

Final volume for all stresses was 20 mL (7:3). The incubation time for all conditions was 24 h at 25 °C. After optimizing all the conditions, the nanoparticles were synthesized in the final volume of 100 mL (70 mL plant extract and 30 mL salt solution). To prepare

the plant extract, 7.5 g algae was taken in 150 mL of dH₂O, and, for the 30 mL salt solution, 8.61 g ZnSO₄ was mixed in 30 mL dH₂O. Then, the absorbance value was measured by using UV–Vis spectrophotometer after an incubation period of 24 h. The stability and biological activity of biogenic nanoparticles are usually influenced by environmental factors such as precursor concentration, contact time or incubation time, pH values, and incubation temperature. Therefore, the optimization of these environmental factors decreases the times required for biosynthesis, increases the NP stability, reduces the NP agglomeration, and finally supports the productivity [43].

3.2.2. Characterization of ZnO-NPs by UV

The production of ZnO-NPs was confirmed by measuring the maximum surface plasmon resonance (SPR) using UV–visible spectroscopy. The morphological characteristics (size and shape), as well as distribution of biogenically synthesized NPs, were usually correlated with SPR. In this respect, the size of the biogenic ZnO-NPs was smaller or larger, according to $300 \leq \text{SPR} \leq 300$. In the current study, the maximum SPR value of the biogenic ZnO-NPs was detected at a wavelength of 310 nm (Figure 3), which confirmed the formation of particles at the nanoscale. The UV–Vis absorption spectrum of the biosynthesized ZnO nanoparticles demonstrated a notable peak at 310 nm, which is most likely a characteristic feature of ZnO-NPs. The obtained results were completely consistent with the efficacy of *Arthrospira platensis*, which is reported to fabricate ZnO-NPs and exhibit intense SPR at 320 nm [38].

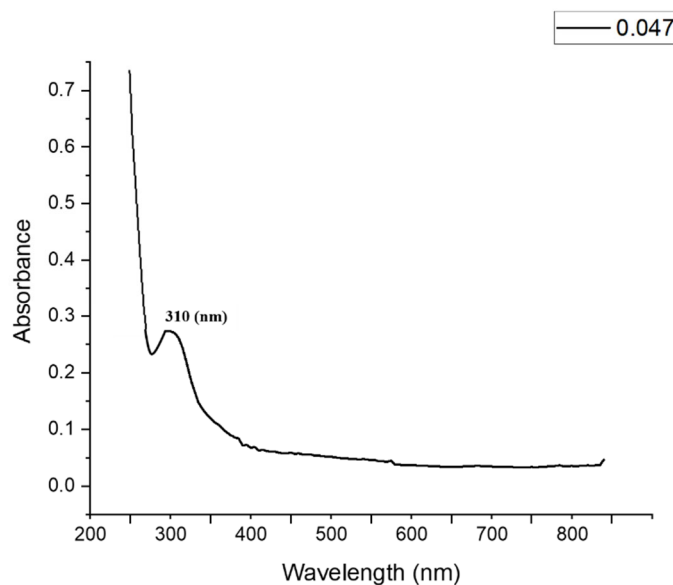


Figure 3. UV–visible spectrum of biosynthesized ZnO-NPs.

3.2.3. Characterization of ZnO-NPs by FT-IR

FT-IR gives the composition and formation of functional groups of the synthesized ZnO nanoparticles (Figure 4). The spectra were collected in absorbance mode at 4 cm⁻¹ spectral resolution, in the 4000–400 cm⁻¹ range. The functional groups were responsible for reducing zinc ions to ZnO, which was observed as bands. Each of the bands corresponded to various stretching modes. Generally, the FT-IR spectrum revealed a complex of bioorganic compounds in algal extract. The FT-IR spectra showed several peaks at different regions. The observed peak of 3600 showed the O–H bond, indicating the presence of alcohols or phenols. The peak detected at 3800 showed O–H, which corresponded to the O–H stretching of the phenolic compounds [44].

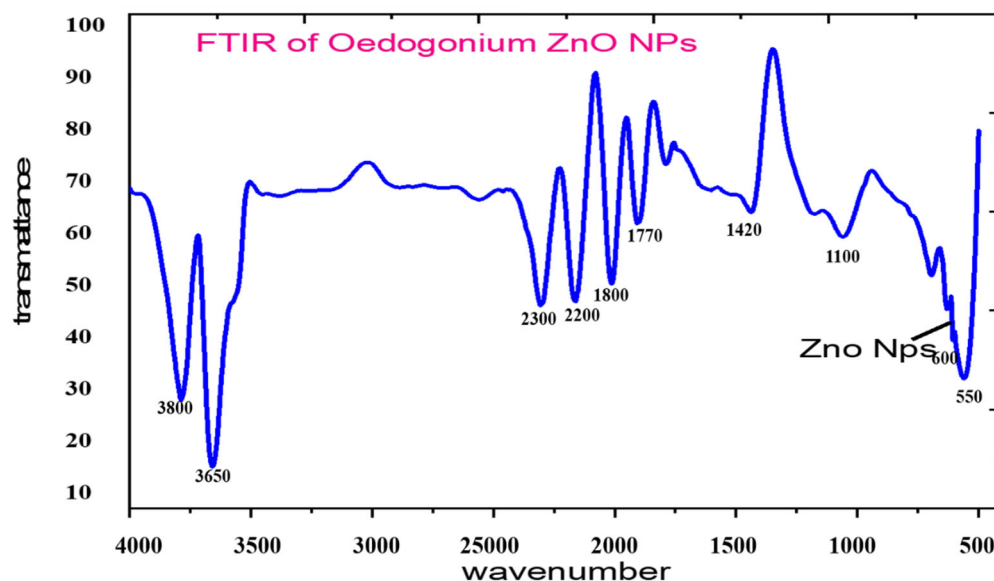


Figure 4. FTIR spectrum of biosynthesized ZnO-NPs.

Additional peaks such as 3650 cm^{-1} , 2300 cm^{-1} , 2200 cm^{-1} , 1800 cm^{-1} , and 1770 cm^{-1} were related to ZnO-NPs. The observed band at 1420 cm^{-1} corresponded to the C–N stretching bond of amino acid, whereas the band observed at wavelength 1100 cm^{-1} may be attributed to the C–O–C ether of the polysaccharides. The band observed at wavelength 1800 cm^{-1} may be attributed to C=C aldehyde or ketone. The absorption wavelength 1770 cm^{-1} was responsible for the vibration bending of the C=O corresponding to the stretching C=O vibration of the proteins or the remaining acetate [38]. The successful formation of ZnO was confirmed by the absorption band observed at 610 cm^{-1} . Consistent with our data, the FT-IR analysis of green synthesized ZnO-NPs showed the ZnO absorption band at wavelength 485 cm^{-1} , 442 cm^{-1} [45], and in the $400\text{ to }500\text{ cm}^{-1}$ range [46], or at wavelength 782 cm^{-1} [47], 450 cm^{-1} , and 600 cm^{-1} [48]. The FT-IR analysis data exhibit the role of the organic substances in *Oedogonium* extract in the reduction, capping, and stabilizations of biosynthesized ZnO-NPs.

3.2.4. Scanning Electron Microscope (SEM)

The structure of ZnO-NPs is illustrated by a scanning electron microscopy technique. SEM provides information about the sample's exterior morphological features, structure, chemical composition, and alignment. The results of the scanning electron microscopy in Figure 5 represent the shape of the nanoparticles made from *Oedogonium* sp. Although different morphological changes were found in the zinc nanoparticles, from spherical to triangular, rod, and circular shapes with variable sizes, i.e., $2\text{ }\mu\text{m}$, $20\text{ }\mu\text{m}$, and $10\text{ }\mu\text{m}$, it was revealed that the nanoparticles agglomerated with the passage of time, forming spherical-shaped particles.

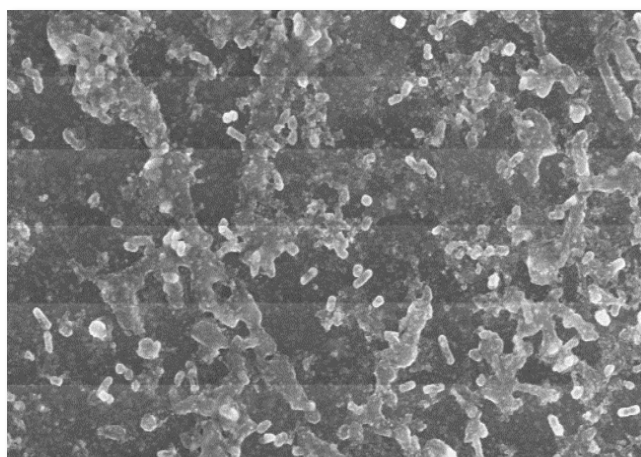


Figure 5. Scanning electron microscope analysis of biosynthesized ZnO-NPs.

3.3. Physicochemical Analysis of Industrial Effluents after 15, 30, and 45 d of Experiment

The optimized nanoparticles were applied in the treatment of leather industry effluents. The four concentrations of effluent, viz. 0%, 5%, 10%, 15%, and 100% (for comparison), were exposed with four different treatments of nanoparticles, 0 (control), 0.1, 0.5, and 1.0 mg. Calculated values after 15 d of treatment showed a significant reduction ($p < 0.05$; LSD test) in all physicochemical parameters including pH, EC, TDS, BOD, COD, etc. (Table 2). With the passage of time, a further reduction in each parameter was recorded after 30 d (Table 3) and 45 d, respectively (Table 4). In four different treatments of NPs, the chloride content was significantly reduced from 1583 to 1312, 1840 to 1613, 2689 to 1511, 3752 to 2731, and 6747 to 5309 mg/L, respectively ($p < 0.05$; LSD test). In 1 mg NPs treatment compared to the control, the BOD values reduced from 39 to 24, 86 to 65, 154 to 110, 373 to 280, and 418 to 370 mg/L (in the 0%, 5%, 10%, 15%, and 100% concentrations). Similarly, COD values were significantly reduced from 135 to 102, 558 to 491, 721 to 502, 950 to 703, and 1120 to 801 mg/L, respectively. The metallic content for Cr, Cd, and Pb was reduced effectively. The Cr content was reduced from 80.4 to 60.9, 164.8 to 117.1, 220.9 to 147.7, and 310.1 to 231.9 mg/L (in the 5%, 10%, and 100% concentrations). Similarly, the Cd content was lowered from 67.5 to 41.9, 120.1 to 98.4, 165.7 to 127.1, and 210.5 to 166.2 mg/L, respectively. Under similar concentrations and treatments, the Pb values were reduced from 25.3 to 16.8, 45.2 to 31.7, 61.9 to 44.1, and 75.5 to 57.3 mg/L, respectively.

Table 2. Changes in physicochemical parameters of different concentrations of leather industry effluents after 15 d of treatment.

NPs Treatment	Effluent Concentration	pH	EC (mS/cm)	TDS (g/L)	Chlorides (mg/L)	BOD (mg/L)	COD (mg/L)	Cr (mg/L)	Cd (mg/L)	Pb (mg/L)
0 mg	0%	6.99 ± 0.12 ^e	0.897 ± 0.09 ^e	0.311 ± 0.06 ^e	39 ± 5.50 ^e	135 ± 3.51 ^e	1583 ± 11.13 ^e	0	0	0
	5%	8.11 ± 0.40 ^d	7.18 ± 0.04 ^d	3.60 ± 0.49 ^d	1840 ± 5.50 ^d	86 ± 5.50 ^d	558 ± 8.02 ^d	80.4 ± 1.74 ^d	67.5 ± 3.95 ^d	25.3 ± 0.90 ^d
	10%	8.55 ± 0.05 ^b	12.00 ± 2.23 ^c	6.65 ± 0.03 ^c	2689 ± 9.01 ^c	154 ± 4.50 ^c	721 ± 3.01 ^c	164.8 ± 2.41 ^c	120.1 ± 1.41 ^c	45.2 ± 2.61 ^c
	15%	8.9 ± 0.18 ^a	17.40 ± 0.45 ^b	8.95 ± 0.60 ^b	3752 ± 5.50 ^b	373 ± 5.51 ^b	950 ± 4.98 ^b	220.9 ± 1.27 ^b	165.7 ± 3.37 ^b	61.9 ± 2.97 ^b
	100%	8.2 ± 0.19 ^c	23.06 ± 0.12 ^a	11.51 ± 0.83 ^a	6747 ± 4.53 ^a	418 ± 2.42 ^a	1120 ± 4.50 ^a	310.1 ± 4.15 ^a	210.5 ± 2.50 ^a	75.5 ± 7.22 ^a
0.1 mg	0%	6.97 ± 0.02 ^d	0.794 ± 0.05 ^e	0.310 ± 0.03 ^a	1551 ± 1.29 ^e	36 ± 1.53 ^e	122 ± 2.35 ^e	0	0	0
	5%	8.09 ± 0.03 ^c	7.01 ± 0.25 ^d	3.42 ± 0.01 ^a	1743 ± 2.65 ^d	79 ± 4.05 ^d	540 ± 4.303 ^d	80.1 ± 1.76 ^d	61.1 ± 2.10 ^d	24.7 ± 1.71 ^d
	10%	8.42 ± 0.06 ^b	11.01 ± 0.41 ^c	6.31 ± 0.03 ^a	2213 ± 2.75 ^c	139 ± 3.05 ^c	651 ± 1.37 ^c	160.1 ± 2.44 ^c	117.2 ± 0.82 ^c	42.1 ± 1.04 ^c
	15%	8.7 ± 0.9 ^a	16.04 ± 0.6 ^b	8.54 ± 0.11 ^a	3432 ± 2.11 ^b	343 ± 2.51 ^b	871 ± 5.10 ^b	212.1 ± 0.63 ^b	159.2 ± 0.94 ^b	58.1 ± 1.57 ^b
	100%	8.15 ± 0.03 ^c	22.1 ± 0.30 ^a	10.77 ± 0.03 ^a	6205 ± 5.03 ^a	402 ± 5.41 ^a	1019 ± 2.08 ^a	301.4 ± 1.02 ^a	205.1 ± 0.94 ^a	71.4 ± 1.02 ^a
0.5 mg	0%	6.95 ± 0.04 ^e	0.789 ± 0.01 ^e	0.301 ± 0.05 ^e	1433 ± 3.51 ^e	29 ± 4.51 ^e	111 ± 3.01 ^e	0	0	0
	5%	8.05 ± 0.05 ^d	6.88 ± 0.06 ^d	3.21 ± 0.05 ^d	1690 ± 7.50 ^d	71 ± 2.94 ^d	519 ± 3.35 ^d	72.4 ± 0.68 ^d	55.3 ± 0.53 ^d	19.8 ± 0.35 ^d
	10%	8.25 ± 0.03 ^b	10.11 ± 0.49 ^c	6.07 ± 0.03 ^c	1803 ± 4.16 ^c	121 ± 3.51 ^c	588 ± 3.51 ^c	145.3 ± 0.58 ^c	109.7 ± 0.31 ^c	38.4 ± 0.45 ^c
	15%	8.55 ± 0.02 ^a	15.22 ± 0.05 ^b	8.07 ± 0.03 ^b	3005 ± 2.01 ^b	310 ± 3.40 ^b	799 ± 4.06 ^b	183.4 ± 0.25 ^b	148.1 ± 0.65 ^b	52.4 ± 0.35 ^b

	100%	8.12 ± 0.35 ^c	20.11 ± 0.03 ^a	10.13 ± 0.06 ^a	5831 ± 1.52 ^a	387 ± 3.05 ^a	905 ± 3.06 ^a	275.1 ± 0.51 ^a	186.3 ± 0.53 ^a	65.7 ± 0.31 ^a
	0%	6.91 ± 0.03 ^c	0.780 ± 0.04 ^e	0.299 ± 0.05 ^e	1312 ± 2.13 ^e	24 ± 2.52 ^e	102 ± 3.51 ^e	0	0	0
	5%	8.0 ± 0.75 ^b	6.80 ± 0.21 ^d	3.01 ± 0.03 ^d	1613 ± 2.51 ^c	65 ± 2.52 ^d	491 ± 3.05 ^d	60.9 ± 0.43 ^d	41.9 ± 0.87 ^d	17.8 ± 0.35 ^d
1 mg	10%	8.1 ± 0.31 ^b	9.81 ± 0.03 ^c	5.82 ± 0.05 ^c	1511 ± 1.53 ^d	110 ± 2.47 ^c	502 ± 3.90 ^c	117.1 ± 0.91 ^c	98.4 ± 0.56 ^c	31.7 ± 0.74 ^c
	15%	8.3 ± 0.25 ^a	13.09 ± 0.04 ^b	7.88 ± 0.04 ^b	2731 ± 5.13 ^b	280 ± 4.58 ^b	703 ± 1.33 ^b	147.7 ± 0.77 ^b	127.1 ± 1.41 ^b	44.1 ± 1.8 ^b
	100%	8.11 ± 0.05 ^b	19.15 ± 0.03 ^a	8.72 ± 0.06 ^a	5309 ± 4.04 ^a	370 ± 4.58 ^a	801 ± 6.56 ^a	231.9 ± 0.41 ^a	166.2 ± 1.01 ^a	57.3 ± 0.23 ^a

Each value mentioned in the table is mean ± SE, and different superscript letters represent the significant difference (LSD $p \leq 0.05$).

Table 3. Changes in physicochemical parameters of different concentrations of leather industry effluents after 30 d of treatment.

NPs Treatment	Effluent Concentration	pH	EC (mS/cm)	TDS (g/L)	Chlorides (mg/L)	BOD (mg/L)	COD (mg/L)	Cr (mg/L)	Cd (mg/L)	Pb (mg/L)
0 mg	0%	6.99 ± 0.12 ^e	0.897 ± 0.09 ^e	0.311 ± 0.06 ^e	39 ± 5.50 ^e	135 ± 3.51 ^e	1583 ± 11.13 ^e	0	0	0
	5%	8.11 ± 0.40 ^d	7.18 ± 0.04 ^d	3.60 ± 0.49 ^d	1840 ± 5.50 ^d	86 ± 5.50 ^d	558 ± 8.02 ^d	80.4 ± 1.74 ^d	67.5 ± 3.95 ^d	25.3 ± 0.90 ^d
	10%	8.55 ± 0.05 ^b	12.00 ± 2.23 ^c	6.65 ± 0.03 ^c	2689 ± 9.01 ^c	154 ± 4.50 ^c	721 ± 3.01 ^c	164.8 ± 2.41 ^c	120.1 ± 1.41 ^c	45.2 ± 2.61 ^c
	15%	8.9 ± 0.18 ^a	17.40 ± 0.45 ^b	8.95 ± 0.60 ^b	3752 ± 5.50 ^b	373 ± 5.51 ^b	950 ± 4.98 ^b	220.9 ± 1.27 ^b	165.7 ± 3.37 ^b	61.9 ± 2.97 ^b
	100%	8.2 ± 0.19 ^c	23.06 ± 0.12 ^a	11.51 ± 0.83 ^a	6747 ± 4.53 ^a	418 ± 2.42 ^a	1120 ± 4.50 ^a	310.1 ± 4.15 ^a	210.5 ± 2.50 ^a	75.5 ± 7.22 ^a
0.1 mg	0%	6.96 ± 0.02 ^d	0.611 ± 0.05 ^e	0.283 ± 0.04 ^e	1354 ± 4.15 ^e	31 ± 3.51 ^e	118 ± 2.51 ^e	0	0	0
	5%	7.5 ± 0.31 ^c	6.59 ± 0.05 ^d	3.08 ± 0.08 ^d	1639 ± 4.50 ^d	75 ± 3.51 ^d	521 ± 3.51 ^d	79.5 ± 0.3 ^d	59.4 ± 0.45 ^d	21.2 ± 0.55 ^d
	10%	7.47 ± 0.06 ^c	9.55 ± 0.05 ^c	5.95 ± 0.12 ^c	1998 ± 3.51 ^c	125 ± 2.51 ^c	615 ± 3.51 ^c	157.1 ± 0.91 ^c	114.5 ± 0.35 ^c	40.3 ± 0.61 ^c
	15%	7.72 ± 0.05 ^b	13.58 ± 0.04 ^b	8.13 ± 0.02 ^b	3115 ± 4.04 ^b	325 ± 3.51 ^b	845 ± 3.52 ^b	208.1 ± 0.51 ^b	155.2 ± 0.56 ^b	55.2 ± 0.91 ^b
	100%	7.91 ± 0.12 ^a	20.37 ± 0.11 ^a	9.52 ± 0.05 ^a	6301 ± 5.03 ^a	351 ± 5.13 ^a	1039 ± 5.50 ^a	297.2 ± 0.95 ^a	197.3 ± 0.61 ^a	68.3 ± 0.6 ^a
0.5 mg	0%	6.93 ± 0.1 ^e	0.553 ± 0.02 ^e	0.251 ± 0.15 ^e	1109 ± 7.54 ^e	27 ± 3.41 ^e	1025.51 ^e	0	0	0
	5%	7.35 ± 0.03 ^d	6.01 ± 0.55 ^d	2.75 ± 0.04 ^d	1502 ± 5.56 ^d	65 ± 3.51 ^d	480 ± 3.05 ^d	66.1 ± 2.23 ^d	52.3 ± 0.52 ^d	19.1 ± 0.91 ^d
	10%	7.3 ± 0.19 ^c	7.41 ± 0.05 ^c	5.37 ± 0.03 ^c	1698 ± 4.51 ^c	112 ± 3.51 ^c	543 ± 3.51 ^c	142.2 ± 0.55 ^c	107.4 ± 0.45 ^c	36.5 ± 0.51 ^c
	15%	7.5 ± 0.35 ^b	10.39 ± 0.04 ^b	7.51 ± 0.05 ^b	2709 ± 4.11 ^b	295 ± 3.51 ^b	705 ± 5.03 ^b	170.6 ± 0.56 ^b	134.7 ± 0.31 ^b	49.7 ± 0.51 ^b
	100%	7.67 ± 0.04 ^a	18.45 ± 0.03 ^a	7.31 ± 0.05 ^a	5713 ± 5.56 ^a	311 ± 4.72 ^a	879 ± 4.33 ^a	251.6 ± 0.55 ^a	172.5 ± 0.51 ^a	61.4 ± 0.56 ^a
1 mg	0%	6.91 ± 0.05 ^e	0.511 ± 0.41 ^e	0.321 ± 0.01 ^e	874 ± 3.46 ^e	20 ± 4.15 ^e	83 ± 4.04 ^e	0	0	0
	5%	7.15 ± 0.07 ^d	5.74 ± 0.08 ^d	2.33 ± 0.06 ^d	1205 ± 5.03 ^d	53 ± 5.56 ^d	447 ± 4.58 ^d	52.5 ± 0.51 ^d	40.5 ± 1.17 ^d	16.4 ± 0.56 ^d
	10%	7.11 ± 1.05 ^c	6.13 ± 0.11 ^c	4.91 ± 0.33 ^c	142.1 ± 0.75 ^c	90 ± 2.36 ^c	451 ± 6.57 ^c	109.7 ± 0.81 ^c	83.3 ± 0.96 ^c	28.2 ± 1.51 ^c
	15%	7.33 ± 0.57 ^b	8.71 ± 1.05 ^b	6.93 ± 1.21 ^b	2153 ± 6.02 ^b	254 ± 5.51 ^b	603 ± 6.65 ^b	102.4 ± 3.74 ^b	113.2 ± 0.95 ^b	42.7 ± 1.61 ^b
	100%	7.51 ± 0.09 ^a	16.01 ± 0.06 ^a	6.73 ± 0.08 ^a	4223 ± 6.02 ^a	295 ± 5.61 ^a	612 ± 5.56 ^a	201.8 ± 0.35 ^a	143.5 ± 0.67 ^a	51.2 ± 1.01 ^a

Each value in this table is mean ± SE, and various superscript letters represent the significant difference (LSD $p \leq 0.05$).

Table 4. Changes in physicochemical parameters of different concentrations of leather industry effluents after 45 d of treatment.

NPs Treatment	Effluent Concentration	pH	EC (mS/cm)	TDS (g/L)	Chlorides (mg/L)	BOD (mg/L)	COD (mg/L)	Cr (mg/L)	Cd (mg/L)	Pb (mg/L)
0 mg	0%	6.99 ± 0.12 ^e	0.897 ± 0.09 ^e	0.311 ± 0.06 ^e	39 ± 5.50 ^e	135 ± 3.51 ^e	1583 ± 11.13 ^e	0	0	0
	5%	8.11 ± 0.40 ^d	7.18 ± 0.04 ^d	3.60 ± 0.49 ^d	1840 ± 5.50 ^d	86 ± 5.50 ^d	558 ± 8.02 ^d	80.4 ± 1.74 ^d	67.5 ± 3.95 ^d	25.3 ± 0.90 ^d
	10%	8.55 ± 0.05 ^b	12.00 ± 2.23 ^c	6.65 ± 0.03 ^c	2689 ± 9.01 ^c	154 ± 4.50 ^c	721 ± 3.01 ^c	164.8 ± 2.41 ^c	120.1 ± 1.41 ^c	45.2 ± 2.61 ^c
	15%	8.9 ± 0.18 ^a	17.40 ± 0.45 ^b	8.95 ± 0.60 ^b	3752 ± 5.50 ^b	373 ± 5.51 ^b	950 ± 4.98 ^b	220.9 ± 1.27 ^b	165.7 ± 3.37 ^b	61.9 ± 2.97 ^b
	100%	8.2 ± 0.19 ^c	23.06 ± 0.12 ^a	11.51 ± 0.83 ^a	6747 ± 4.53 ^a	418 ± 2.42 ^a	1120 ± 4.50 ^a	310.1 ± 4.15 ^a	210.5 ± 2.50 ^a	75.5 ± 7.22 ^a
0.1 mg	0%	6.94 ± 1.02 ^c	0.551 ± 0.01 ^e	0.271 ± 0.01 ^a	1252 ± 5.68 ^e	29 ± 4.51 ^e	111 ± 3.56 ^e	0	0	0
	5%	7.05 ± 0.13 ^b	5.02 ± 0.50 ^d	2.95 ± 0.05 ^a	1573 ± 2.11 ^d	71 ± 4.58 ^d	504 ± 6.24 ^d	75.4 ± 0.62 ^d	57.1 ± 1.05 ^d	19.5 ± 0.51 ^d
	10%	6.93 ± 0.05 ^c	7.35 ± 0.67 ^c	5.12 ± 0.53 ^a	1901 ± 5.03 ^c	121 ± 3.83 ^c	555 ± 3.51 ^c	154.5 ± 0.66 ^c	110.2 ± 1.01 ^c	38.7 ± 0.83 ^c
	15%	7.3 ± 0.38 ^{bc}	12.39 ± 1.19 ^b	7.31 ± 0.75 ^a	3012 ± 5.31 ^b	318 ± 3.51 ^b	812 ± 4.04 ^b	185.3 ± 2.05 ^b	151.1 ± 4.95 ^b	53.7 ± 1.19 ^b
	100%	7.45 ± 0.53 ^a	18.37 ± 0.77 ^a	9.14 ± 0.94 ^a	6044 ± 3.05 ^a	335 ± 4.11 ^a	923 ± 3.91 ^a	290.4 ± 4.51 ^a	190.2 ± 4.25 ^a	65.3 ± 0.85 ^a
0.5 mg	0%	6.92 ± 1.02 ^b	0.521 ± 0.04 ^e	0.243 ± 0.05 ^e	954 ± 3.05 ^e	23 ± 3.81 ^e	95 ± 2.92 ^e	0	0	0
	5%	6.9 ± 0.38 ^b	4.87 ± 0.04 ^d	2.52 ± 0.08 ^d	1237 ± 4.26 ^d	60 ± 2.92 ^d	465 ± 1.71 ^d	61.2 ± 1.41 ^c	45.7 ± 2.24 ^d	16.9 ± 1.28 ^d
	10%	6.85 ± 0.74 ^c	6.01 ± 0.06 ^c	4.31 ± 0.04 ^c	1447 ± 2.51 ^c	103 ± 2.89 ^c	423 ± 2.41 ^c	132.7 ± 0.63 ^b	91.5 ± 1.09 ^c	31.1 ± 1.01 ^c
	15%	6.91 ± 0.05 ^b	9.99 ± 0.13 ^b	6.93 ± 0.02 ^b	2419 ± 1.73 ^b	258 ± 3.39 ^b	673 ± 1.44 ^b	127.9 ± 0.29 ^b	127.3 ± 1.04 ^b	41.8 ± 0.78 ^b
	100%	7.3 ± 0.16 ^a	15.25 ± 0.11 ^a	7.03 ± 0.27 ^a	5017 ± 1.21 ^a	275 ± 1.77 ^a	704 ± 1.71 ^a	235.2 ± 0.83 ^a	149.3 ± 0.64 ^a	52.5 ± 0.31 ^a
1 mg	0%	6.9 ± 0.37 ^b	0.481 ± 0.04 ^e	0.201 ± 0.03 ^e	712 ± 1.89 ^e	18 ± 1.84 ^e	68 ± 1.69 ^e	0	0	0
	5%	6.8 ± 0.14 ^d	4.25 ± 0.06 ^d	2.01 ± 0.08 ^d	877 ± 1.39 ^d	41 ± 1.36 ^d	385 ± 1.91 ^d	31.7 ± 0.61 ^d	30.3 ± 0.24 ^d	9.9 ± 0.14 ^d
	10%	6.85 ± 0.02 ^c	5.02 ± 0.12 ^c	3.14 ± 0.04 ^c	1097 ± 1.41 ^c	78 ± 2.39 ^c	318 ± 2.28 ^c	69 ± 1.35 ^c	52.4 ± 0.84 ^c	18.3 ± 0.45 ^c

15%	6.91 ± 0.03 ^b	7.99 ± 0.01 ^b	5.37 ± 0.02 ^b	1939 ± 1.88 ^b	195 ± 1.51 ^b	423 ± 2.46 ^b	95.4 ± 0.68 ^b	72.3 ± 0.88 ^b	28.3 ± 1.34 ^b
100%	7.32 ± 0.01 ^a	11.39 ± 0.02 ^a	6.17 ± 0.13 ^a	3812 ± 0.69 ^a	193 ± 1.88 ^a	521 ± 1.51 ^a	142.6 ± 0.76 ^a	89.1 ± 0.59 ^a	30.7 ± 0.61 ^a

Each value in this table is mean of 3 replicates, and various superscript letters represent the significant difference (LSD $p \leq 0.05$).

Table 5. Percentage removal of physiochemical parameters of tannery effluents by using ZnO-NPs.

NPs Treatment	pH	EC (mS/cm) (%)	TDS (%)	Chlorides (%)	BOD (%)	COD (%)	Cr (%)	Cd (%)	Pb (%)
After 15 d of Treatment									
0.1	1.0	4.24	6.67	8.07	4.28	9.26	2.80	2.56	5.43
0.5	1.09	12.86	12.21	13.61	7.85	19.41	11.28	11.49	12.98
1	1.33	17.02	24.43	21.34	11.90	28.67	25.21	21.04	24.10
After 30 d of Treatment									
0.1	3.65	11.74	17.50	9.61	16.42	17.80	4.15	6.27	9.53
0.5	6.57	20.06	36.65	15.36	25.95	21.72	18.86	18.05	18.67
1	8.52	30.63	41.68	37.43	29.76	45.50	34.92	31.82	32.18
After 45 d of Treatment									
0.1	9.25	20.40	20.79	10.45	20.23	19.41	6.35	9.64	13.50
0.5	10.84	33.92	39.08	25.67	34.52	37.31	24.15	29.07	30.46
1	11.08	50.64	46.53	43.52	54.04	53.60	54.01	57.67	59.33

The chloride content decreased from 132 to 83, 549 to 447, 718 to 90, 946 to 603, and 1115 to 612 mg/L (under five different concentrations, respectively, and NPs treatment) after 30 d. At the concentration ranges of 0%, 5%, 10%, 15%, and 100% and treatment stresses of 0 (control), 0.1, 0.5, and 1 mg, the BOD values decreased from 38 to 20, 85 to 53, 152 to 90, 360 to 254, and 405 to 295 mg/L, respectively. Using the same sequence, the calculated values of COD were also significantly reduced ($p < 0.05$; LSD test), from 132 to 83, 549 to 447, 718 to 451, 946 to 603, and 1115 to 612 mg/L, respectively. The effective reduced metallic content for Cr was 52.5, 109.7, 102.4, and 201.8 mg/L at 5%, 10%, 15%, and 100%, respectively. Calculated values were 40.4, 83.3, 113.2, and 143.5 mg/L for Cd and 17.4, 31.2, 42.7, 51.2 mg/L for Pb, respectively.

All physicochemical parameters were further reduced to about 2.5 times the pre-treatment values, suggesting the efficient removal of heavy metals with ZnO nanoparticles ($p < 0.05$; LSD test; Table 5). Maximum removal was noted under the treatment of 1 mg at the concentrations of 5%, 10%, 15%, and 100%, respectively. Chloride content removal was in the following order: 1553 to 712, 1830 to 877, 2671 to 1097, 3742 to 1939, and 6740 to 3812 mg/L, respectively. The calculated BOD and COD values under the treatment of 0 (control), 0.1, 0.5, and 1 mg NPs and at the concentrations of 0%, 5%, 10%, 15% and 100% were 36 to 18, 83 to 41, 149 to 78, 351 to 195, and 402 to 193 mg/L and 130 to 68, 542 to 385, 714 to 318, 941 to 423, and 1112 to 521 mg/L, respectively. Although the values of all parameters were increased with the increases in effluent concentrations, in comparison to the same concentration under different stresses of nanoparticles, all values were reduced significantly ($p < 0.05$). The ZnO-NPs showed their maximum adsorption capability for metals in the following order: Cr > Cd > Pb. The reduced values for Cr, Cd, and Pb were 142.6, 89.1, and 30.7 mg/L, respectively, after 45 d.

4. Discussion

Nanotechnology is a promising and advanced field of science particularly for treating wastewater effluents. Green synthesis of nanoparticles from algal resources is cost-effective due to their high surface area, high reactivity, and strong mechanical properties that are highly efficient and effective for wastewater treatment related to tannery effluents [30].

The synthesis of nanoparticles was observed by the initial color change of *Oedogonium* sp., from light green to pale yellow. Physicochemical parameters such as pH, EC, TDS, chlorides, BOD, COD, and heavy metals (Cr, Cd, and Pb) were also monitored, along with different treatments. The calculated values in pretreatment effluents were as follows: pH 8.21, EC 23.08 mS cm⁻¹, TDS 11.54 mg/L, BOD 420 mg/L, COD 1123 mg/L, Cl⁻ 6750 mg/L, Cd 210.5 mg/L, Cr 310.1 mg/L, and Pb 75.5 mg/L. Some macrophytes and algal species effectively reduced pollutants from industry effluents with a substantial reduction in pH (6.97, 6.97, and 6.42 in the case of macrophytes and 6.46, 6.59, and 6.34 in the case of algal species) with the passage of time (i.e., after 1, 2, and 3 d of incubation) [49]. Although in this study, the pH levels began to lower down with time, the lowest values were recorded after 45 d of incubation at 5% and under the treatment of 1 mg NPs. It is also suggested that increases in chemical treatment may differentially influence physiochemical parameters such as pH, EC, and COD [50]. Using different doses of FeCl₃ as the coagulant showed that increases in treatment dose did not reduce the EC levels from tannery effluents. Contrary to previous findings, the present study showed an effective reduction in EC burden from different concentration of effluents. Precisely, the application of 1 mg NPs at 15%, reduced the EC value from 17.58 mg/L to 13.09, 8.71, and 5.37 mg/L after 15, 30, and 45 d, respectively [51]. Our results suggest that biosynthesized ZnO nanoparticles efficiently reduced the EC content compared to the chemical approach. The bioremediation potential of ZnO nanoparticles toward the reduction in TDS content was good enough compared to that of a revolving algal bioreactor [31]. In another study, researchers used such reactors to lower the burden of TDS from wastewater, and the technique proved to be 27% efficient [52]. In the present study, 53% of removal efficiency for TDS content was found at 100% concentration for the leather tanning industry, with a significant reduction in values from 11.54 mg/L to 8.72, 6.73, and 6.17 mg/L after 15, 30, and 45 d, respectively, at 1 mg nanoparticle treatments. A further 5% reduction in TDS content was observed before and after the experiment. Moreover, a significant reduction in chloride content was achieved at 5% effluent concentration and 1 mg of ZnO nanoparticles. At 10%, the effluent load of the chloride reduction was within permissible limits (about 1000 mg/L Cl⁻) but at 15% and 100% the values were higher than the permissible limits. The precipitation method was applied at a pH range of 6–11 and a temperature of 30 °C. The amount of biochemical oxygen demand (BOD) was reduced at the 1 mg treatment and 5% effluent concentration (65, 53, and 41 mg/L) after 15, 30, and 45 d of treatment, respectively, and a further reduction in BOD was recorded at 10% and 15%. In the current study, the reduced COD content at the 1 mg treatment and 100% was 801, 612, and 521 mg/L after 15, 30, and 45 d of treatment, respectively. Similar reduction in chemical oxygen demand was observed in other concentrations of leather industrial effluents [50].

The interaction of heavy metals with nanoparticles resulted in the variation in adsorption of heavy metal content in a study conducted by [53]. The results showed the potentially higher removal efficiency of Cu²⁺, Ag⁺, and Pb²⁺ and the lower removal efficiency of Cr⁴⁺, Mn²⁺, Cd²⁺, and Ni²⁺ in the presence of nanoparticles. In the current research, green synthesized ZnO nanoparticles showed maximum adsorption for Cr, Cd, and Pb in a similar sequence. Chromium was reduced to 60.9, 52.5, and 26.1 mg/L after 15, 30, and 45 d, respectively, at 5% effluent concentration. About 48% Cr reduction was observed after 7 d of treatment in *Phragmites australis* [54]. In the present investigation, the reduction in Cd content was ~42, 40.5, and 23.5 mg/L at 5%; 98.4, 83.3, and 42.4 mg/L at 10%; and 127.1, 113.2, and 57.4 mg/L at 15% after 15, 30, and 45 d, respectively. A similar reduction in cadmium levels by ZnO-NPs was reported by [51]. Pb concentration was reduced from 25.3 mg/L to 17.8, 16.4, and 9.9 mg/L at a concentration of 5%. At 100%, the content was

reduced to 57.3, 51.2, and 25.7 mg/L [51]. The bio-sorption of Pb was aided by using indigenous microorganisms under applied stress for about 20 d, which significantly reduced the lead content in the sample [55]. Iron oxide NPs remove 90% of Cr from tannery effluent [56]. MgO-NPs have the potential to reduce TSS (98%), TDS (98%), BOD (89%), COD (97%), and Cr (from 835 mg/L to 21 mg/L; 97%) in tanning effluent [57]. Similarly, a study reported that the green synthesis of MgO-NPs from *Rhizopus oryzae* reduced TSS (97%), TDS (98%), BOD (87%), COD (95%), and Cr (98%) in tanning effluent [58]. These findings indicate that the biologically mediated synthesis of nanoparticles could become a useful resource in removing pollutants. The phytochemicals present in algae (as well as plant extracts) may also increase the antibacterial, antifungal, and anticancer properties of green-synthesized nanostructures, by generating a synergetic nanostructure that combines the antimicrobial properties of both the plant extract and the NPs themselves [59].

In the present study, heavy metals were significantly reduced in all industrial effluent concentrations, and the removal efficiency for all parameters was optimized after 45 d of treatment with 1 mg nanoparticles. The green synthesis of zinc oxide nanoparticles showed effective bioremediation against leather industry effluents. The removal percentages of tannery effluents may be attributed to the adsorption of heavy metals onto the adsorption sites present on the NPs surface [60]. Nanomaterials are utilized as adsorbents that depend upon structural qualities including good specificity for the use of eliminating heavy metal ions from wastewater at low concentrations. Agglomeration of nanoparticles with the passage of time (such as in this study) may be ideally helpful for the adsorption of toxic substances or other pollutants, as they could elevate the surface-region to volume proportion [61]. The adsorption processes are governed by the diffusion of metals to the pores fixed on the adsorbent surface, which reacts with the surface active sites. The high adsorption of ZnO-NPs could also be attributed to the liberation of OH⁻ from Zn(OH)₂, which forms as a result of the hydration process of ZnO [62].

Adsorption is a simple physicochemical method used to purify harmful wastewaters from heavy metals. In this specific case, surface adsorption onto solid sorbents takes place through electrostatic forces. These can be caused, for example, by hydroxyl groups and/or other functional groups, resulting in a positively or negatively charged sorbent surface. Depending on the charge of the contaminants to be removed, oppositely charged adsorbents are applied. The efficiency of the adsorption is characterized by chemical interactions on the surface of the adsorbents. The main parameters influencing adsorption are pH, temperature, stirring duration (i.e., contact time), initial concentration of the substance to be adsorbed, and the adsorbent dosage. In the case of heavy metal adsorption, adsorbents such zinc oxide nanoparticles (ZnO-NPs) have been investigated, which selectively interact with Cr. In batch experiments, ZnO-NPs exhibited very high affinity toward Cr³⁺, with an optimum pH range of 3–7 and a very short contact time of 20 min. It is worth mentioning that the author also showed that ZnO-NPs selectively adsorbed Cr³⁺ from wastewater, which contained a mixture of heavy metals, including Ni²⁺, Pb²⁺, Cu²⁺, and Cr³⁺. Other important heavy metals to be removed by adsorption from wastewater are cadmium (Cd²⁺) and lead. The initial pH is a driving factor for successful adsorption, as initial pH influences the deprotonation of the adsorbents, which favors enhanced adsorption in a suitable pH range by reducing the repulsion of metal cations (i.e., electrostatic interactions). This mechanism is based not only on electrostatic interaction but also on metal coordination and complexation, which interact with and provide synergetic effects that result in enhanced adsorption and finally increased removal efficiency. Metal coordination and especially complexation strongly depend on the pH. The pH also influences the precipitation of metals. The authors stated that organic matter did not negatively affect the adsorption capacity, but the nitrogen content of the wastewater significantly reduced the capacity of the adsorbent.

Our findings showed that application of the ZnO nanoparticle could help with reducing toxic substances in the wastewater effluents of the leather industry to safe levels and at a reasonable cost, as the conventional methods of remediation may cost from USD

10 to 1000 per cubic meter. The costs for remediation, especially for groundwater, are very high. The American Environmental Protection Agency (EPA) estimated, in 2004, costs of about USD 250 billion for remediation, including construction and post-construction activities, by several cleanup programs only in the United States. The production of ZnO nanoparticles was very prospective. The technical analysis of producing 250 kg of ZnO nanoparticles per day shows the total cost of the equipment to be USD 21,450.00. Such an investment will be profitable after more than three years. This project can compete with payback period (PBP) capital market standards because of the short-term investment returns. To ensure the feasibility of such a project, the project should be estimated from the ideal conditions to the worst case for production, including labor, sales, raw materials, utilities, and external conditions. In the synthesis of ZnO-NPs, zinc sulphate, algal extract, and distal water are used with an algal extract and zinc sulphate ratio of 7:3. Moreover, the conversion rate for the zinc oxide formation process is 100%. Nevertheless, the ZnO-NPs material are successfully applied to real wastewater and show proof for routine application.

5. Conclusions

The present study highlights the capability of nanoparticles for reducing the pollution load from tannery effluents. The study indicates that ZnO nanoparticles optimize their maximum adsorption capacity for heavy metals and for some other physicochemical parameters after 45 d of treatment, particularly at low concentrations. Owing to the efficacy of NPs, it could prove to be a cost-effective and eco-friendly process.

The trend of nanomaterials for water-pollutant treatment is rapidly increasing in this modern era, due to the limited water supply at the global level. Innovative techniques such as the use of ZnO-NPs could provide good quality water for drinking purposes, besides removing pollutants. Nanotechnology for water purification is an alternative approach for the availability of fresh water, though it requires operational digital monitoring techniques. There is a need to synthesize modified nanomaterials that should be effective, have high efficiency, and be easy to handle and eco-friendly. In view of the above-mentioned findings, the use of ZnO-NPs could prove to be a cost-effective technology for wastewater treatment.

Author Contributions: Conceptualization, S.A.K.; Data curation, M.H. and Z. A. S. ; Formal analysis, N.M., M.H. and Z.A.S. Conceptualization, data analysis, original drafting, A.A.E.-H. and H.-H.Y.; review & editing, funding acquisition; S.A.K. and A.M.J.; Project administration, B.A. and M.I.H.; Writing—original draft, review & editing; B.A.; Writing—review & editing, N.M., I.A., Z.A. and M.I.H. All authors have read and agreed to the published version of the manuscript.

Funding: The authors extend their appreciation to the Researchers Supporting Project number (PNURSP2022R75), Princess Nourah bint Abdulrahman University, Riyadh, Saudi Arabia.

Institutional Review Board Statement: Not applicable.

Informed Consent Statement: Not applicable.

Data Availability Statement: Not applicable.

Acknowledgments: Princess. The authors extend their appreciation to the Researchers Supporting Project Number (PNURSP2022R75), Princess Nourah bint Abdulrahman University, Riyadh, Saudi Arabia

Conflicts of Interest: The authors declare no conflict of interest.

Abbreviations

CNTs	Carbon nano tubes
As	Arsenic
Pb	Lead
Cd	Cadmium

Zn	Zinc
Cu	Copper
CAS	Conventional activated sludge
SPR	Surface plasmon resonance
EC	Electrical conductivity
TDS	Total dissolved solid
GO	Graphene oxide
RGO	Reduced graphene oxide
NMs	Nanomaterials
NPs	Nanoparticles
ZnO	Zinc oxide
SNHS	Silica nano hollow sphere
NPANI	Nanopolyaniline
SDS	Sodium dodecyl sulfate
nZVI	Nano zero valent iron
MSA	Mercaptoethylamino acid
HMO	Hydrous manganese oxide
MgO	Magnesium oxide
HNO ₃	Nitric acid
EDTA	Ethylene diamintetraacetic acid
EBT	Eriochrome Black T
AAS	Atomic absorption spectrophotometer

References

- Emparan, Q.; Jye, Y.S.; Danquah, M.K.; Harun, R. Cultivation of *Nannochloropsis* sp. microalgae in palm oil mill effluent (POME) media for phycoremediation and biomass production: Effect of microalgae cells with and without beads. *J. Water Process Eng.* **2020**, *33*, 101043.
- Adel, M.; Saravi, H.N.; Dadar, M.; Niyazi, L.; Ley-Quinonez, C.P. Mercury, lead, and cadmium in tissues of the Caspian Pond Turtle (*Mauremys caspica*) from the southern basin of Caspian Sea. *Environ. Sci. Pollut. Res.* **2017**, *24*, 3244–3250.
- Abd El-Mageed, T.A.; El-Sherif, A.M.A.; Abd El-Mageed, S.A.; Abdou, N.M. A novel compost alleviate drought stress for sugar beet production grown in Cd-contaminated saline soil. *Agric. Water Manag.* **2019**, *226*, 105831.
- Qadri, H.; Bhat, R.A. The concerns for global sustainability of freshwater ecosystems. In *Fresh Water Pollution Dynamics and Remediation*; Springer: Berlin/Heidelberg, Germany, 2020; pp. 1–13.
- Zhao, G.; Li, H.; Yang, Y.; Zhao, Q.; Su, T.; Ma, J. Facile one-step synthesis of PhC₂Cu nanowires with enhanced photocatalytic performance. *Res. Sq.* **2022**. <https://doi.org/10.21203/rs.3.rs-1536066/v1>.
- Barros, M.U.G.; Wilson, A.E.; Leitão, J.I.R.; Pereira, S.P.; Buley, R.P.; Fernandez-Figueroa, E.G.; Capelo-Neto, J. Environmental factors associated with toxic cyanobacterial blooms across 20 drinking water reservoirs in a semi-arid region of Brazil. *Harmful Algae* **2019**, *86*, 128–137.
- Kotresha, K.; Mohammed, S.A.S.; Sanaulla, P.F.; Moghal, A.A.B.; Moghal, A.A.B. Evaluation of Sequential Extraction Procedure (SEP) to Validate Binding Mechanisms in Soils and Soil-Nano-Calcium Silicate (SNCS) Mixtures. *Indian Geotech. J.* **2021**, *51*, 1069–1077.
- Rodrigues, J.; Inzé, D.; Nelissen, H.; Saibo, N.J.M. Source–sink regulation in crops under water deficit. *Trends Plant Sci.* **2019**, *24*, 652–663.
- Mohammed, S.A.S.; Moghal, A.A.B. Nanomaterials-based solidification/stabilization of metal-contaminated soils. In *Nanomaterials for Soil Remediation*; Elsevier: Amsterdam, The Netherlands, 2021; pp. 385–407.
- Murtaza, B.; Amjad, M.; Shahid, M.; Imran, M.; Shah, N.S.; Abbas, G.; Naem, M.A. Compositional and health risk assessment of drinking water from health facilities of District Vehari, Pakistan. *Environ. Geochem. Health* **2020**, *42*, 2425–2437.
- Rajput, N.L.; Mughal, M.A.; Balouch, A.; Khan, K.M.; Tunio, S.A.; Kanwal; Sohu, S. Effective photocatalytic methylene orange dye degradation ability in coloured textile contaminated water by highly efficient catalyst Schiff-based resin-encapsulated supported on TiO₂@ SiO₂ metal oxide nanoparticles. *Int. J. Environ. Anal. Chem.* **2020**, *102*, 3561–3575.
- Hussain, R.; Khattak, S.A.; Ali, L.; Sattar, S.; Zeb, M.; Hussain, M.L. Impacts of the linear flowing industrial wastewater on the groundwater quality and human health in Swabi, Pakistan. *Environ. Sci. Pollut. Res.* **2021**, *28*, 56741–56757.
- Ilyas, M.; Ahmad, W.; Khan, H.; Yousaf, S.; Yasir, M.; Khan, A. Environmental and health impacts of industrial wastewater effluents in Pakistan: A review. *Rev. Environ. Health* **2019**, *34*, 171–186.
- Yasin, G.; Rahman, S.U.; Yousaf, M.T. Bin; Azhar, M.F.; Zahid, D.M.; Imtiaz, M.; Hussain, B. Phytoremediation Potential of *E. camaldulensis* and *M. alba* for Copper, Cadmium, and Lead Absorption in Urban Areas of Faisalabad City, Pakistan. *Int. J. Environ. Res.* **2021**, *15*, 597–612.

15. Munir, N.; Hasnain, M.; Roessner, U.; Abideen, Z. Strategies in improving plant salinity resistance and use of salinity resistant plants for economic sustainability. *Crit. Rev. Environ. Sci. Technol.* **2021**, *52*, 2150–2196.
16. Silambarasan, S.; Logeswari, P.; Vangnai, A.S.; Cornejo, P. Rhodotorula mucilaginosa CAM4 improved selenium uptake in *Spinacia oleracea* L. and soil enzymatic activities under abiotic stresses. *Environ. Sci. Pollut. Res.* **2022**, *52*, 2150–2196. <https://doi.org/10.1007/s11356-022-21935-y>.
17. Amini, E.; Babaei, A.; Mehrnia, M.R.; Shayegan, J.; Safdari, M.-S. Municipal wastewater treatment by semi-continuous and membrane algal-bacterial photo-bioreactors. *J. Water Process Eng.* **2020**, *36*, 101274.
18. Aghilinategh, M.; Barati, M.; Hamadani, M. Supercritical methanol for one pot biodiesel production from chlorella vulgaris microalgae in the presence of CaO/TiO₂ nano-photocatalyst and subcritical water. *Biomass Bioenergy* **2019**, *123*, 34–40.
19. Kiss, É. Nanotechnology in food systems: A review. *Acta Aliment.* **2020**, *49*, 460–474.
20. Lowry, G. V.; Avellan, A.; Gilbertson, L.M. Opportunities and challenges for nanotechnology in the agri-tech revolution. *Nat. Nanotechnol.* **2019**, *14*, 517–522.
21. He, X.; Deng, H.; Hwang, H. The current application of nanotechnology in food and agriculture. *J. Food Drug Anal.* **2019**, *27*, 1–21.
22. El-Kassas, H.Y.; Ghobrial, M.G. Biosynthesis of metal nanoparticles using three marine plant species: Anti-algal efficiencies against “*Oscillatoria simplicissima*”. *Environ. Sci. Pollut. Res.* **2017**, *24*, 7837–7849.
23. Dharmaprabakaran, T.; Karthikeyan, S.; Periyasamy, M.; Mahendran, G. Combustion analysis of CuO₂ nanoparticle addition with blend of botryococcus braunii algae biodiesel on CI engine. *Mater. Today Proc.* **2020**, *33*, 2874–2876.
24. Hasnain, M.; Abideen, Z.; Naz, S.; Roessner, U.; Munir, N. Biodiesel production from new algal sources using response surface methodology and microwave application. *Biomass Convers. Biorefin.* **2021**. <https://doi.org/10.1007/s13399-021-01560-4>.
25. Almomani, F. Algal cells harvesting using cost-effective magnetic nano-particles. *Sci. Total Environ.* **2020**, *720*, 137621.
26. Kaliamurthi, S.; Selvaraj, G.; Cakmak, Z.E.; Korkmaz, A.D.; Cakmak, T. The relationship between *Chlorella* sp. and zinc oxide nanoparticles: Changes in biochemical, oxygen evolution, and lipid production ability. *Process Biochem.* **2019**, *85*, 43–50.
27. Jang, H.J.; Lee, M.H.; Lee, E.J.; Yang, X.; Kong, I.C. Toxicity Evaluation of Metals and Metal-oxide Nanoparticles based on the Absorbance, Chlorophyll Content, and Cell Count of *Chlorella vulgaris*. *Clean Technol.* **2017**, *23*, 27–33.
28. Puay, N.-Q.; Qiu, G.; Ting, Y.-P. Effect of Zinc oxide nanoparticles on biological wastewater treatment in a sequencing batch reactor. *J. Clean. Prod.* **2015**, *88*, 139–145.
29. Schwab, F.; Bucheli, T.D.; Lukhele, L.P.; Magrez, A.; Nowack, B.; Sigg, L.; Knauer, K. Are carbon nanotube effects on green algae caused by shading and agglomeration? *Environ. Sci. Technol.* **2011**, *45*, 6136–6144.
30. Mahuwala, A.A.; Hemant, V.; Meharwade, S.D.; Deb, A.; Chakravorty, A.; Grace, A.N.; Raghavan, V. Synthesis and characterisation of starch/agar nanocomposite films for food packaging application. *IET Nanobiotechnol.* **2020**, *14*, 809–814.
31. Siddiqi, K.S.; ur Rahman, A.; Husen, A. Properties of zinc oxide nanoparticles and their activity against microbes. *Nanoscale Res. Lett.* **2018**, *13*, 141.
32. Kondzior, P.; Butarewicz, A. Effect of heavy metals (Cu and Zn) on the content of photosynthetic pigments in the cells of algae *Chlorella vulgaris*. *J. Ecol. Eng.* **2018**, *19*, 18–28.
33. Pirzadah, T.B.; Malik, B.; Salam, S.T.; Ahmad Dar, P.; Rashid, S. Impact of heavy metal stress on plants and the role of various defense elements. *Iran. J. Plant Physiol.* **2019**, *9*, 2883–2900.
34. Munir, N.; Sharif, N.; Naz, S.; Saleem, F.; Manzoor, F. Harvesting and processing of microalgae biomass fractions for biodiesel production (a review). *Sci. Technol. Dev.* **2016**, *32*, 235–243.
35. Kumar, D.; Abdul Rub, M.; Akram, M.; Kabir-ud-Din Interaction of chromium (III) complex of glycylphenylalanine with ninhydrin in aqueous and cetyltrimethylammonium bromide (CTAB) micellar media. *Tenside Surfactants Deterg.* **2014**, *51*, 157–163.
36. Wani, P.A.; Wahid, S.; Khan, M.S.A.; Rafi, N.; Wahid, N. Investigation of the role of chromium reductase for Cr (VI) reduction by *Pseudomonas* species isolated from Cr (VI) contaminated effluent. *Biotechnol. Res. Innov.* **2019**, *3*, 38–46.
37. Hussain, M.; Raja, N.I.; Iqbal, M.; Ejaz, M.; Aslam, S. Green synthesis and evaluation of silver nanoparticles for antimicrobial and biochemical profiling in Kinnow (*Citrus reticulata* L.) to enhance fruit quality and productivity under biotic stress. *IET Nanobiotechnol.* **2019**, *13*, 250–256.
38. El-Belely, E.F.; Farag, M.; Said, H.A.; Amin, A.S.; Azab, E.; Gobouri, A.A.; Fouda, A. Green synthesis of zinc oxide nanoparticles (ZnO-NPs) using *Arthrospira platensis* (Class: Cyanophyceae) and evaluation of their biomedical activities. *Nanomaterials* **2021**, *11*, 95.
39. Agarwal, H.; Kumar, S.V.; Rajeshkumar, S. A review on green synthesis of zinc oxide nanoparticles—An eco-friendly approach. *Resour. Technol.* **2017**, *3*, 406–413.
40. Lashin, I.; Fouda, A.; Gobouri, A.A.; Azab, E.; Mohammedsaleh, Z.M.; Makharita, R.R. Antimicrobial and in vitro cytotoxic efficacy of biogenic silver nanoparticles (Ag-NPs) fabricated by callus extract of *Solanum incanum* L. *Biomolecules* **2021**, *11*, 341.
41. APHA-AWWA-WPCF. *Standard Methods for the Examination of Water and Wastewater*; APHA American Public Health Association: Washington, DC, USA, 1981.
42. Hseu, Z.-Y. Evaluating heavy metal contents in nine composts using four digestion methods. *Bioresour. Technol.* **2004**, *95*, 53–59.
43. Mohd Yusof, H.; Mohamad, R.; Zaidan, U.H.; Rahman, A. Microbial synthesis of zinc oxide nanoparticles and their potential application as an antimicrobial agent and a feed supplement in animal industry: A review. *J. Anim. Sci. Biotechnol.* **2019**, *10*, 57.

44. Abdo, A.M.; Fouda, A.; Eid, A.M.; Fahmy, N.M.; Elsayed, A.M.; Khalil, A.M.A.; Alzahrani, O.M.; Ahmed, A.F.; Soliman, A.M. Green Synthesis of Zinc Oxide Nanoparticles (ZnO-NPs) by *Pseudomonas aeruginosa* and Their Activity against Pathogenic Microbes and Common House Mosquito, *Culex pipiens*. *Materials* **2021**, *14*, 6983.
45. Nagarajan, S.; Arumugam Kuppasamy, K. Extracellular synthesis of zinc oxide nanoparticle using seaweeds of gulf of Mannar, India. *J. Nanobiotechnol.* **2013**, *11*, 39.
46. Zhang, G.; Shen, X.; Yang, Y. Facile synthesis of monodisperse porous ZnO spheres by a soluble starch-assisted method and their photocatalytic activity. *J. Phys. Chem. C* **2011**, *115*, 7145–7152.
47. Singh, J.; Kaur, S.; Kaur, G.; Basu, S.; Rawat, M. Biogenic ZnO nanoparticles: A study of blueshift of optical band gap and photocatalytic degradation of reactive yellow 186 dye under direct sunlight. *Green Process. Synth.* **2019**, *8*, 272–280.
48. Fakhari, S.; Jamzad, M.; Kabiri Fard, H. Green synthesis of zinc oxide nanoparticles: A comparison. *Green Chem. Lett. Rev.* **2019**, *12*, 19–24.
49. Jahan, M.A.A.; Akhtar, N.; Khan, N.M.S.; Roy, C.K.; Islam, R.; Nurunnabi, M. Characterization of tannery wastewater and its treatment by aquatic macrophytes and algae. *Bangladesh J. Sci. Ind. Res.* **2014**, *49*, 233–242.
50. Fettig, J.; Pick, V.; Oldenburg, M.; Phuoc, N. V Treatment of tannery wastewater for reuse by physico-chemical processes and a membrane bioreactor. *J. Water Reuse Desalin.* **2017**, *7*, 420–428.
51. Chowdhury, M.; Mostafa, M.G.; Biswas, T.K.; Saha, A.K. Treatment of leather industrial effluents by filtration and coagulation processes. *Water Resour. Ind.* **2013**, *3*, 11–22.
52. Peng, J.; Kumar, K.; Gross, M.; Kunez, T.; Wen, Z. Removal of total dissolved solids from wastewater using a revolving algal biofilm reactor. *Water Environ. Res.* **2020**, *92*, 766–778.
53. Le, A.T.; Pung, S.-Y.; Sreekantan, S.; Matsuda, A. Mechanisms of removal of heavy metal ions by ZnO particles. *Heliyon* **2019**, *5*, e01440.
54. García-Valero, A.; Martínez-Martínez, S.; Faz, Á.; Terrero, M.A.; Muñoz, M.Á.; Gómez-López, M.D.; Acosta, J.A. Treatment of Wastewater from the Tannery Industry in a Constructed Wetland Planted with *Phragmites australis*. *Agronomy* **2020**, *10*, 176.
55. Abioye, O.P.; Oyewole, O.A.; Oyeleke, S.B.; Adeyemi, M.O.; Orukotan, A.A. Biosorption of lead, chromium and cadmium in tannery effluent using indigenous microorganisms. *Braz. J. Biol. Sci.* **2018**, *5*, 13–24.
56. Guan, X.; Chang, J.; Chen, Y.; Fan, H. A magnetically-separable Fe₃O₄ nanoparticle surface grafted with polyacrylic acid for chromium (III) removal from tannery effluents. *RSC Adv.* **2015**, *5*, 50126–50136.
57. Saied, E.; Eid, A.M.; Hassan, S.E.-D.; Salem, S.S.; Radwan, A.A.; Halawa, M.; Saleh, F.M.; Saad, H.A.; Saied, E.M.; Fouda, A. The catalytic activity of biosynthesized magnesium oxide nanoparticles (MgO-NPs) for inhibiting the growth of pathogenic microbes, tanning effluent treatment, and chromium ion removal. *Catalysts* **2021**, *11*, 821.
58. Hassan, S.E.-D.; Fouda, A.; Saied, E.; Farag, M.; Eid, A.M.; Barghoth, M.G.; Awad, M.A.; Hamza, M.F.; Awad, M.F. *Rhizopus oryzae*-mediated green synthesis of magnesium oxide nanoparticles (MgO-NPs): A promising tool for antimicrobial, mosquitocidal action, and tanning effluent treatment. *J. Fungi* **2021**, *7*, 372.
59. Gunalan, S.; Sivaraj, R.; Rajendran, V. Green synthesized ZnO nanoparticles against bacterial and fungal pathogens. *Prog. Nat. Sci. Mater. Int.* **2012**, *22*, 693–700.
60. Fouda, A.; Hassan, S.E.-D.; Abdel-Rahman, M.A.; Farag, M.M.S.; Shehal-deen, A.; Mohamed, A.A.; Alsharif, S.M.; Saied, E.; Moghanim, S.A.; Azab, M.S. Catalytic degradation of wastewater from the textile and tannery industries by green synthesized hematite (α -Fe₂O₃) and magnesium oxide (MgO) nanoparticles. *Curr. Res. Biotechnol.* **2021**, *3*, 29–41.
61. Mallikarjunaiah, S.; Pattabhiramaiah, M.; Metikurki, B. Nanotechnology for Food, Agriculture and Environment. In *Application of Nanotechnology in the Bioremediation of Heavy Metals and Wastewater Management*; Springer: Berlin/Heidelberg, Germany, 2020; pp. 297–321.
62. Fouda, A.; Hassan, S.E.-D.; Saied, E.; Hamza, M.F. Photocatalytic degradation of real textile and tannery effluent using biosynthesized magnesium oxide nanoparticles (MgO-NPs), heavy metal adsorption, phytotoxicity, and antimicrobial activity. *J. Environ. Chem. Eng.* **2021**, *9*, 105346.